

INFRARED MEASUREMENT OF THE TEMPERATURE DISTRIBUTION OF A REPETITIVELY PULSED ELECTRON BEAM EXTRACTION FOIL AS A BEAM UNIFORMITY DIAGNOSTIC\*

M. T. Buttram, J. W. Ginn and G. S. Phipps  
Sandia National Laboratories  
P. O. Box 5800  
Albuquerque, NM 87185

Summary

This paper presents results of experiments to measure the current extracted through the foil of an electron beam diode by observing the heating of the foil. Generally anode current density is measured with a dosimeter film, often of dubious linearity, or with Faraday cups which give a current density versus time map at isolated points or with an array of calorimeters. For the present measurements a fast scanning infrared camera is used to measure the temperature rise of the foil after a pulse. The measurement takes 600  $\mu$ s for a single line scan or 16 ms for a full raster scan. Resolution is comparable to that of dosimeter film, the IR camera is easily calibrated to produce accurate temperature plots, and because of the fast scan this system is ideally suited to observing small scale structure in the beam current density for repetitive pulses up to several hundred Hertz pulse repetition rates.

Introduction

Frequently the foil temperature is of greater interest than the current density. For example when a beam is extracted repetitively heat buildup in the anode foil limits the total power per area that can be extracted. A measurement of temperature versus position and time shows hot spots due to nonuniform beam generation and gives a measurement of the effectiveness of whatever anode cooling may be employed. Foil temperature may be converted directly to the product of beam current density times time (coulombs per  $\text{cm}^2$ ) provided the voltage is constant during the pulse and the spectrum of angles for the beam is known. Generally the angles of incidence are near normal because the beam must pass through a support structure ("Hibachi") to reach the anode. Since the incidence angle affects the heating of the foil in proportion to the secant, the effect is second order (i.e., small) for angles near normal and will be neglected. Care was taken in the data to be presented to work with a square voltage pulse.

Energy is deposited in the anode foil by (1)  $dE/dx$  losses, (2) back scatter from the material beyond the foil, and (3) electrons back scattered into the diode by the anode foil which are subsequently returned to the foil by the diode field. These effects were simulated using the electron-photon transport code CYLTRAN.<sup>1</sup> The results are almost identical to the  $dE/dx$  losses as calculated in Reference 2 except at the lowest energies. Using these losses and the thermal properties of the foil it is possible to calculate the temperature rise in a foil for given voltage and current density waveforms. Data will be presented for titanium foils 0.0025 cm thick. For a 250 keV beam assuming a 20° divergence 21% of the beam energy or 0.4  $\text{J}/\text{cm}^2$  is deposited in the foil. This causes a 71°C temperature rise per pulse.

Cooling may be accomplished by radiation, conduction to the anode support, convection to the

material beyond the foil, and conduction to the material beyond the foil with a phase change in that material. Radiation and conduction to the supports are far less effective than even moderate convection. Conduction with a phase change would be very effective but has not been tried. Convection cooling may be modeled as turbulent flow over a flat plate when the geometry of Figure 1 is used. The cooling rate  $dQ/dt$  ( $\text{cal}/\text{cm}^2/\text{s}$ ) is given by

$$\frac{dQ}{dt} = \frac{d}{dt} (C \rho X T) = -h (T - T_0) \quad (1)$$

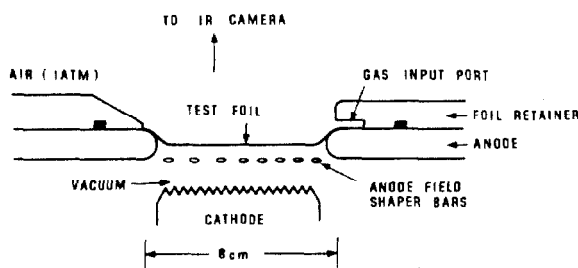


Figure 1. Schematic of the experiment.

The foil variables are specific heat  $C$ , density  $\rho$ , thickness  $X$ , and temperature  $T$ . Gas parameters are temperature  $T_0$  and cooling coefficient  $h$ . Foil temperature decays exponentially with a characteristic time

$$\tau = C \rho X / h \quad (2)$$

Generally  $h$  is in the range 0.003 to 0.03  $\text{J}/\text{cm}^2/\text{s}/^\circ\text{K}$ . For a 0.0025 cm thick titanium foil  $\tau = 0.4$  to 0.04 s.

The particular model of convective flow over a flat plate used gives<sup>3</sup>

$$h = 0.036 u^{0.8} L^{-0.2} \left[ \frac{\rho_g}{\mu} \right]^{0.8} (Pr)^{1/3} k_g \quad (3)$$

The quantity in brackets is a dimensionless number involving only properties of the gas, density ( $\rho_g$ ), viscosity ( $\mu$ ), Prandtl number ( $Pr$ ) and conductivity ( $k_g$ ). It is tabulated as  $F$  in Table I for three common gases. Note that even though the parameters vary considerably from gas-to-gas  $F$  is relatively constant.  $L$ , the distance from the gas nozzle, has little effect on  $h$  because it enters to a small power. The dominant effect is due to gas velocity  $u$ . Inserting an average value for  $F$

$$h = 5.9 \times 10^{-4} v^{0.8} L^{-0.2} \text{ J}/\text{s}/\text{cm}^2/^\circ\text{K} \quad (4)$$

for  $v$  in m/s and  $h$  in meters. At 150 m/s (500 ft/s) and  $L = 0.3$  m,  $h$  is 0.04  $\text{J}/\text{cm}^2/\text{s}/^\circ\text{K}$  which is in the range referred to previously as being typical and  $\tau = 42$  ms.

If the foil is repetitively pulsed at a period  $t_0$  with a temperature rise per pulse of  $\Delta T$  then after  $N$  pulses the temperature is

$$T - T_0 = \Delta T e^{-t/T} (1 + e^{-t_0/T} + e^{-2t_0/T} + \dots + e^{-Nt_0/T}) \quad (5)$$

\*This work was supported by the U.S. Department of Energy, under Contract DE-AC04-76-DP00789 and the Air Force Weapons Laboratory.

TABLE I  
Thermal Properties of Cooling Gases

	Air (100°F)	He (200°F)	CO <sub>2</sub> (100°F)
$\rho \left( \frac{\text{lb mass}}{\text{ft}^3} \right)$	0.071	0.008	0.108
$\mu \left( \frac{\text{lb mass}}{\text{ft-s}} \right)$	$1.285 \times 10^{-5}$	$1.48 \times 10^{-5}$	$1.05 \times 10^{-5}$
$P_c$	0.72	0.686	0.77
$k \left( \frac{\text{BTU}}{\text{hr ft}^2 \text{ } ^\circ\text{F}} \right)$	0.0154	0.097	0.01
$F$	13.61	13.1	14.9

Here  $t$  is the time since the most recent pulse. This may be summed to give

$$\frac{T - T_0}{\Delta T} = e^{-t/\tau} \left( \frac{1 - e^{-Nt_0/\tau}}{1 - e^{-t_0/\tau}} \right) \quad (6)$$

Asymptotically the peak temperature rise is  $\Delta T / (1 - e^{-t_0/\tau}) \sim \Delta T \tau / t_0$  for  $\tau \gg t_0$ . This temperature buildup is the most common cause of anode foil failure in high power electron beam diodes.

### Experimental Results

To study beam extraction in the range of 250 A/cm<sup>2</sup> at 250 kV which were the parameters of interest a small area (~8 cm<sup>2</sup>) diode was built for the RTF-1<sup>4</sup> pulser. RTF-1 is a 10 Ω, 30 ns (2 way time) coaxial pulse forming line pulser which operates to 350 kV on the cable at rates to 100 Hz for up to 10<sup>6</sup> shots in some runs. A water resistor served to terminate the cable in its characteristic impedance assuring a square voltage pulse to the high impedance (~50 Ω) diode which paralleled the resistor. Voltage was measured with a dV/dt monitor and current with a 0.35 Ω shunt (CVR) which observed the current through the diode only. Typical waveforms are shown in Figure 2. The voltage rises to 250 kV in 7 ns and has a 22 ns flat top. The shape of the current waveform is determined by the cathode.

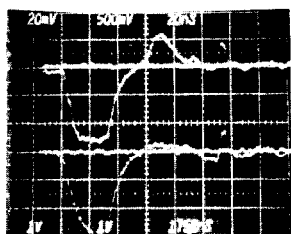


Figure 2. Waveforms at 200 ns/div, upper trace voltage (160 kV/div), lower trace diode current (4.6 kA/div).

Several cathodes were explored in an attempt to get a uniform electron beam at the anode foil with a rapid turn on. Table II lists the main candidates used. Current density is proportional to the diode voltage (in MV) to the 3/2 power and inversely proportional to the A-K spacing. Values of the proportionality constant  $K$  are given in the table. In the interest of maintaining a reasonably large A-K gap a large  $K$  was desirable. Carbon felt, with the largest  $K$ , gave a very filamented beam so a grooved brass plate, shown schematically in Figure 1 was used. Uniformity, current turn on and lifetime of the brass cathode were acceptable.

Test foils were mounted in the holder shown schematically in Figure 1. The extraction area was

TABLE II  
Properties of Cathodes

Cathode	K	d for 250 A/cm <sup>2</sup> at 0.25 MV	Uniformity
0.5 mil SS Blade	260	0.36 cm	acceptable
21 mil Brass Blade	396	0.44	acceptable
2 x 0.5 mil SS Blades	534	0.52	acceptable
9 Saw Blades	690	0.59	acceptable
Grooved Brass Plate	1065	0.73	acceptable (~ ± 15%)
Carbon Felt	1209	0.78	poor

1 cm across by 8 cm high. The foil surface was approximately 1 cm behind the remainder of the anode. The anode field shaper bars were used to keep the beam from diverting to the foil support. Cooling gas was blown along the length of the foil from a manifold at one end. Air, argon, and sulfur hexafluoride were used. Gas velocity was estimated from the measured flow rate and checked with a Pitot tube. Temperature was measured along a single line through the center of the foil along the long dimension. It was measured with a scanning IR camera<sup>5</sup> which was selectable for a single scan every 600 μs or a full raster scan every 16 ms. The camera was calibrated using titanium and aluminum foils heated to temperatures in the range of interest. A typical calibration curve for camera output voltage versus temperature is given in Figure 3. The camera is rather sensitive for all but the lowest temperatures for titanium foils (emissivity = 0.3) but for lower emissivity ( $\epsilon = 0.055$ ) aluminum foils single shot temperature rises ( $\Delta T \sim 60^\circ\text{C}$ ) were masked by noise.

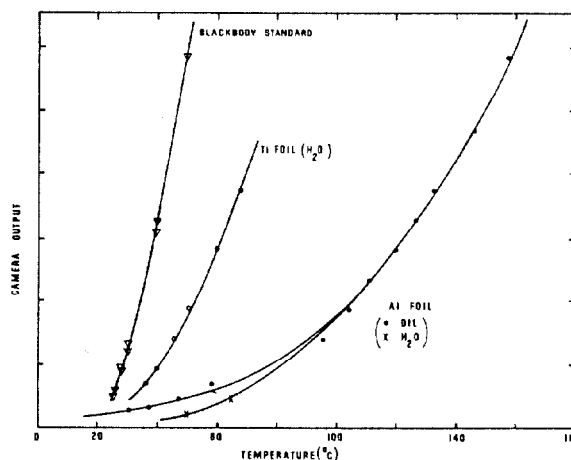


Figure 3. Calibration curves for the IR camera.

Figure 4 shows the maximum foil temperature versus time along the line of scan for a single pulse on titanium at 250 A/cm<sup>2</sup>, 250 kV, 30 ns. The expected temperature rise is 71°C, the measured rise is 70°C. In general the measured rise is in the range 65 to 75°C in good agreement with the calculations indicating that the temperature profiles may be used to measure current density profiles. A fit of temperature decay to an exponential yields a decay time for each combination of cooling gas and velocity. This is plotted in Figure 5. Argon and air lie on a common curve as expected from earlier arguments, sulfur hexafluoride provides better cooling. The cooling coefficient for air and argon varies as velocity to the 0.9 power, consistent within errors to the 0.8 expected. The power for sulfur hexafluoride is 1.2.

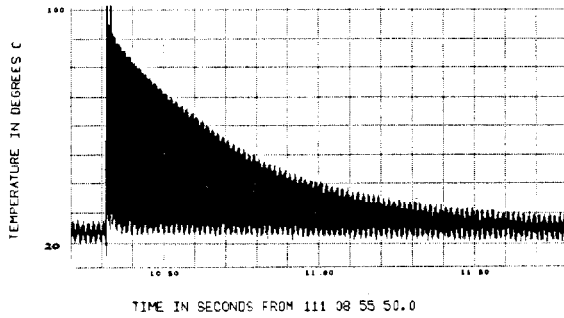


Figure 4. Temperature vs. time for a single pulse.

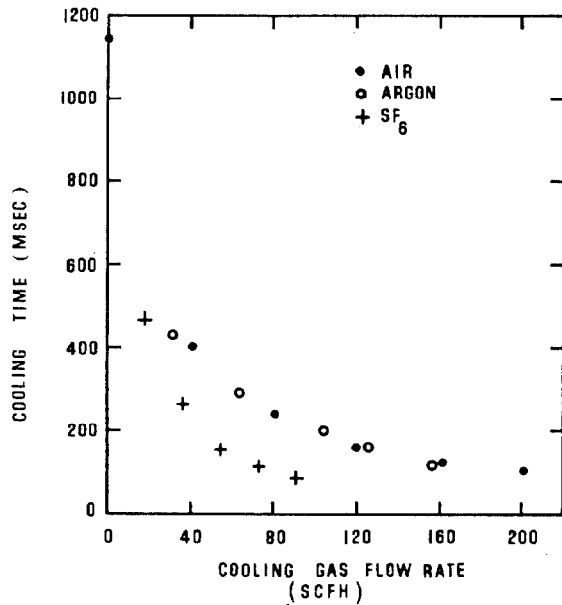


Fig. 5. Cooling time vs. gas flow rate.

Figure 6 displays the temperature versus position along the foil for a single pulse. The structure on the temperature distribution correlates directly to the structure of the anode field shaper bar. The positions of the bars are marked by the arrows in Figure 6. The camera spatial resolution is better than the bar width which was 0.075 cm. The relative emission from various parts of the cathode was observed to change with accumulated pulses.

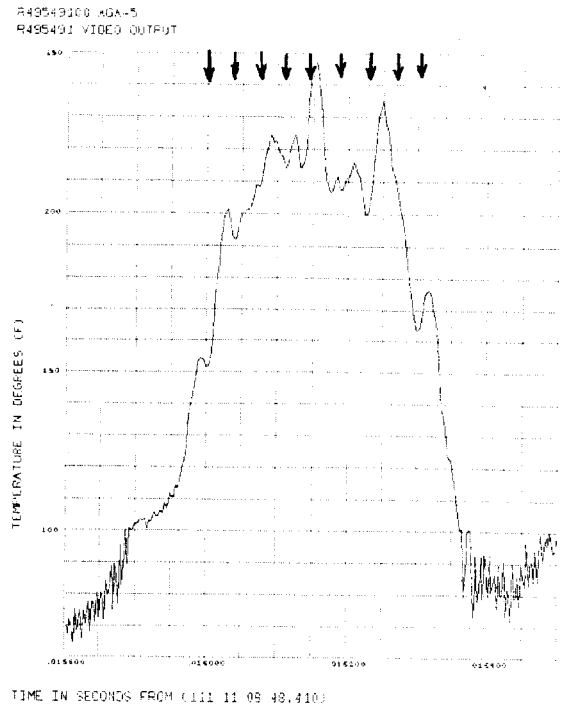


Figure 6. Foil temperature distribution immediately following a pulse.

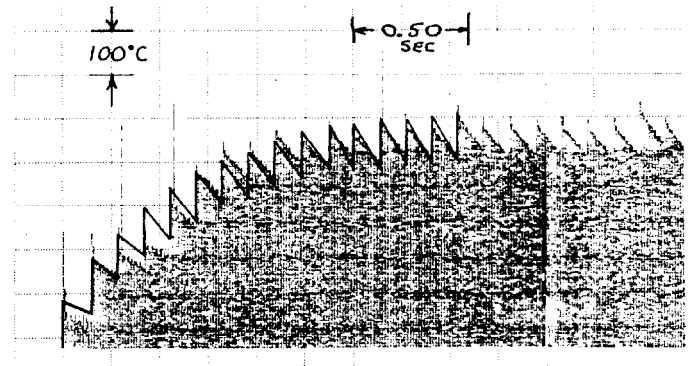


Figure 7. Foil temperature vs. time under repetitive pulsing at 10 Hz.

Figure 7 shows the buildup of foil temperature as a function of time for a 5 second run at 10 Hz. Equation (6) is used to compute the temperature versus time line drawn on the rising part of the figure. The large spikes appearing on several pulses (such as the first 3) are at present unexplained but may be related to an interaction of EMP from the accelerator with the camera. Figure 7 illustrates the ability of this technique to follow a train of pulses and measure shot-to-shot uniformity.

#### Conclusions

It has been shown that a scanning IR camera can be used to measure spatial and temporal temperature profiles along the extraction foil of an electron beam diode. From this data the extraction current density can be inferred. The temperature distribution can also be used to study foil cooling and explore foil failure mechanisms.

#### References

1. "Cyltran: A Cylindrical-Geometry Multi-material Electron/Photon Monte Carlo Transport Code", J. A. Halbleib and W. H. VanDevender, Sandia Report SAND74-0030, 1975.
2. Studies in the Penetration of Charged Particles in Matter, National Academy of Sciences-National Research Council, Pub. 1134, Washington, DC, 1964.
3. Principles of Heat Transfer, F. Kreith, International Textbook Co., Scranton, PA, 1966.
4. M. T. Buttram and G. J. Rohwein, IEEE Transactions on Electron Devices, Vol. ED-26, No. 10, October 1979.
5. AGA Model 680 Thermovision Infrared Camera.